Prevalence of radio jets associated with quasar outflows and feedback

Miranda E. Jarvis[1,2]

[1]Max-Planck Institut fûr Astrophysik, Karl-Schwarzschild-Str. 1, 85741 Garching, Germany
email: mjarvis@eso.org

[2]European Southern Observatory, Karl-Schwarzschild-Str. 2, 85748 Garching, Germany

Abstract. We have identified that radio jets are commonly associated with "radiative mode" feedback in quasars. By performing a systematic multi-wavelength study of $z < 0.2$ quasars, we have found that 70–80% of our sample of 'radio-quiet' type 2 quasars, which host kpc-scale ionized gas outflows, exhibit radio jet structures. Here, we discuss our results on the pilot sample of 10 objects that combine high resolution ($\sim$0.25-1 arcsec) radio imaging at 1-7 GHz with optical IFU observations. Our results demonstrate that it is extremely common for jets to be spatially and kinematically linked to kpc-scale ionized gas kinematics in such quasars. Therefore, radio jets may be an important driver of outflows during 'radiative mode' feedback, apparently blurring the lines between the traditional divisions of feedback modes.

Keywords. galaxies: active –galaxies: evolution – galaxies: jets – quasars: emission lines

1. Introduction

The mechanisms by which AGN influence the gas of their host galaxies (feedback) are often split into two categories: the 'quasar' or 'radiative' mode, where radiation pressure dominates the feedback, and the 'jet' or 'radio' mode, where the majority of the AGN's energy is in a relativistic jet (see e.g., Heckman & Best 2014; Fabian 2012). In particular, the exact mechanism by which 'quasar' mode AGN interact with their host galaxies has been widely studied with little consensus, with radiative winds, compact jets and star formation all suggested (see e.g. Condon *et al.* 2013; Mullaney *et al.* 2013; Zakamska & Greene 2014). However, much of the previous observational work has lacked the spatial resolution to unambiguously distinguish between these possibilities. Our current work seeks to shed additional light on this problem by using high spatial resolution ($\sim$1kpc) radio images of 10 'radio-quiet' quasars, and in so doing we have found that the division between quasar and jet mode feedback might not be as sharp as has previously been believed. This work is presented in full in Jarvis *et al.* (2019).

2. Sample properties

The ten quasars discussed here were selected from our parent sample of $24\,264$ $z < 0.4$ AGN, that were spectroscopically identified as AGN from SDSS (DR7; Abazajian *et al.* 2009). We selected type 2 ('obscured') AGN with $z < 0.2$, with 'quasar' like luminosities ($\log L_{\mathrm{AGN}} = 45$–$46[\,\mathrm{erg\,s^{-1}}]$), and a luminous broad [O III] component, indicative of a powerful ionised outflow (i.e., a broad component that contributes $\geq$30% of the total flux and has a full width at half-maximum FWHM$>700\,\mathrm{km\,s^{-1}}$; Mullaney *et al.* 2013). In Harrison *et al.* (2014), we found large scale ($\gtrsim$kpc) ionised outflows in all 10 AGN, using Gemini-South GMOS (Gemini Multi-Object Spectrograph) IFS data.

All of our targets were detected by the FIRST survey (Becker *et al.* 1995) with moderate radio luminosities ($\log L_{1.4\,\mathrm{GHz}} =23.2$–$24.4[\,\mathrm{W\,Hz^{-1}}]$) and are either unresolved or
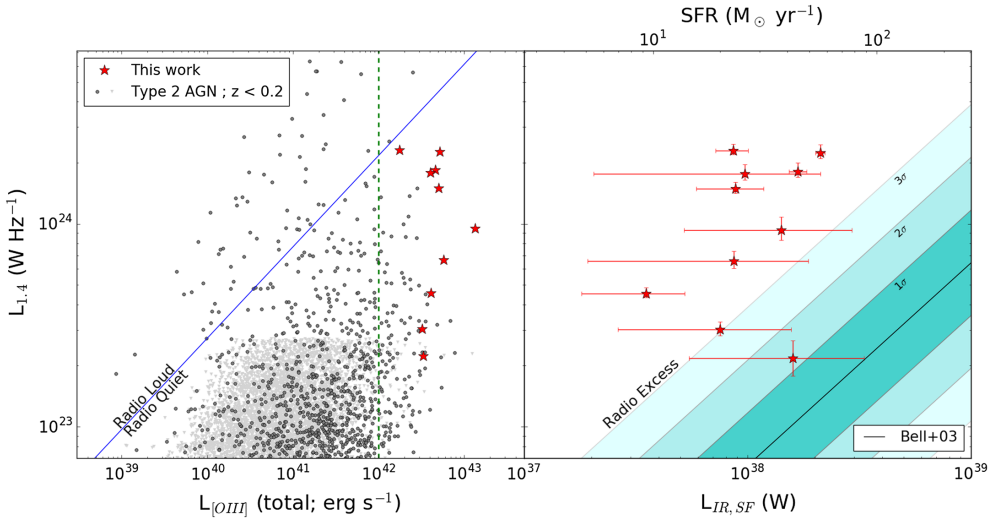
Figure 1. Left: Radio versus [O III] luminosity for our galaxies (red stars), with the division between "radio-loud" and "radio-quiet" from Xu *et al.* (1999) (blue line) and our parent sample of type 2 AGN with $z < 0.2$ (black points, grey for upper limits; Mullaney *et al.* 2013). Our selection criterion of $L_{[OIII]} > 10^{42}$ erg s^{-1} is shown by a dashed green line. Right: The FIR-radio correlation of Bell (2003) compared to the values for our primary sample. We take $L_{IR,SF}$ from the luminosity of the dust component from UV-FIR SED fitting. The solid black line is the average correlation from Bell (2003), with the cyan regions marking 1, 2 and 3σ regions respectively. Although all of our targets are classified as radio-quiet by most traditional methods, all but one appear to have excess radio emission above what is predicted from star formation.

marginally resolved at FIRST's ∼5″ resolution (see Harrison *et al.* 2014). They are all classified as 'radio-quiet' using the separation criteria of Xu *et al.* (1999) (see Figure 1) and 'star formation dominated' by the separation criteria of Best & Heckman (2012). However, we find that all but one of our targets have a radio excess from what would be expected from their star formation alone. We determined this by using the infrared–radio correlation for normal star forming galaxies from Bell (2003) and UV-FIR SED fitting to isolate the infrared luminosity due to star formation from the AGN contribution (see Figure 1; Jarvis *et al.* 2019). This provides initial evidence for non star formation processes (likely AGN) producing the majority of the radio emission in our sources.

3. Observations

We present radio images from our observing campaigns with the Karl G. Jansky Very Large Array (VLA) in the L and C-bands with A and B configurations and the enchanced Multi-Element Radio Linked Interferometer Network (*e*MERLIN) that were designed to obtain high resolution (i.e., ≈0.3–1″; ≈ 600 pc at a representative redshift of $z = 0.1$) 1–7 GHz radio images of these targets. We compared the radio images to the ionized gas outflow properties traced by [O III] in our GMOS (Harrison *et al.* 2014) and VIMOS observations (Harrison *et al.* 2015 and Jarvis *et al.* 2019). We fit the [O III] line profile with multiple Gaussians to reduce the effect of noise and measure the kinematic properties of the ionized gas in all pixels (Harrison *et al.* 2014). Specifically, in Figure 2 we show the signal-to-noise ratio (S/N) of [O III] with radio contours from our VLA C-band A configuration data (0.3″ beam) and where needed to show additional morphological features the *e*MERLIN (0.3″ beam) and VLA C-band B-configuration data (1″ beam)†.

† For J1338+1503 we only have VLA C-band B configuration data
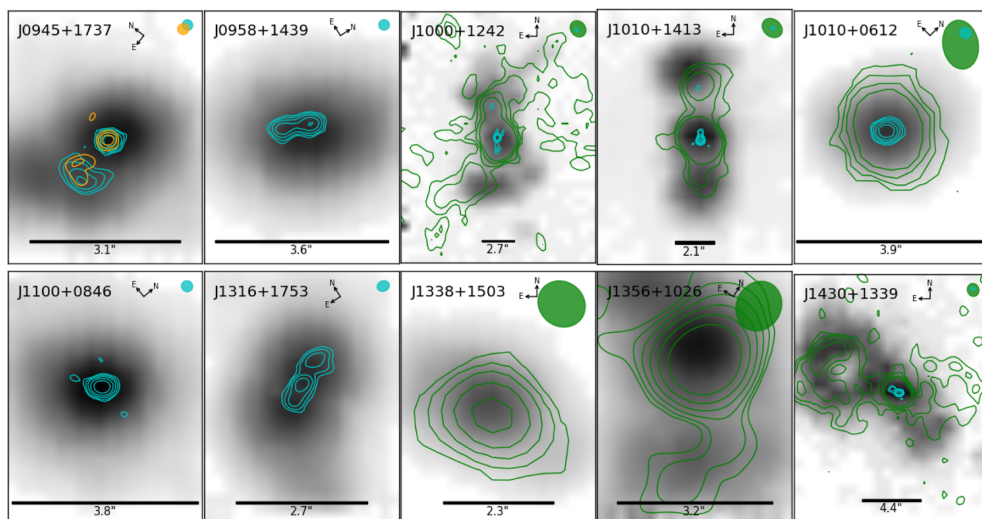
Figure 2. The distribution of [O III] emission (S/N maps) with contours overlaid from our radio images. Specifically, our VLA C-band B-configuration data is shown in green, VLA C-band A-configuration data in cyan and *e*MERLIN in orange. The beam for each radio image is shown as an appropriately coloured ellipse in the top right corner. The scale bar in each is 7kpc long. We observe a close connection between the radio and ionised gas morphologies.

4. Results and conclusions

Perhaps surprisingly for a 'radio-quiet' sample, 70–80% show distinct, collimated morphological features in the radio on 1–25 kpc scales (for one target, J1338+1503, we cannot rule out the presence of ∼kpc scale features due to the lack of high resolution radio images). For three sources in particular (J0945+1737, J1000+1242 and J1010+1413) the high resolution images reveal elongated jet like components and flat spectrum ($\alpha > -0.2$) compact components. These latter structures, identified in the high-resolution images, are embedded in low resolution lobes, and we suggest that the most viable interpretation is that they are hot-spots from a jet. Furthermore, the sizes and lumionsities of our sources in the radio are comparable to the low luminosity population of compact steep spectrum (CSS) and Fanaroff-Riley type I (FRI) radio galaxies (see e.g. An & Baan 2012), suggesting a possible continuity between radio-loud and radio-quiet populations and supporting our interpretation that the collimated structures we identify are due to jets. Finally, these jets are in all cases coincident with kinematically disturbed ionised gas, an example of which can be seen in Figure 3. The combination of ionized gas kinematics and radio morphologies suggests that the jets and gas are interacting with each other, with the jet possibly driving outflows and the gas possibly deflecting the jets (see e.g. Leipski & Bennert 2006; Jarvis *et al.* 2019). We note that shallow, low-resolution radio images such as those from the FIRST survey are insufficient to unambiguously determine the origin of the radio emission or the driving mechanism of the outflows in typical quasars, even at these low redshifts. Our observations support a scenario where compact radio jets, with modest radio luminosities, are a crucial feedback mechanism for massive galaxies during the quasar phase. In our future work, we will explore the impact of these jets on the molecular (star forming) gas through a recently accepted ALMA proposal and extend the sample to 42 objects, through newly acquired VLA images.
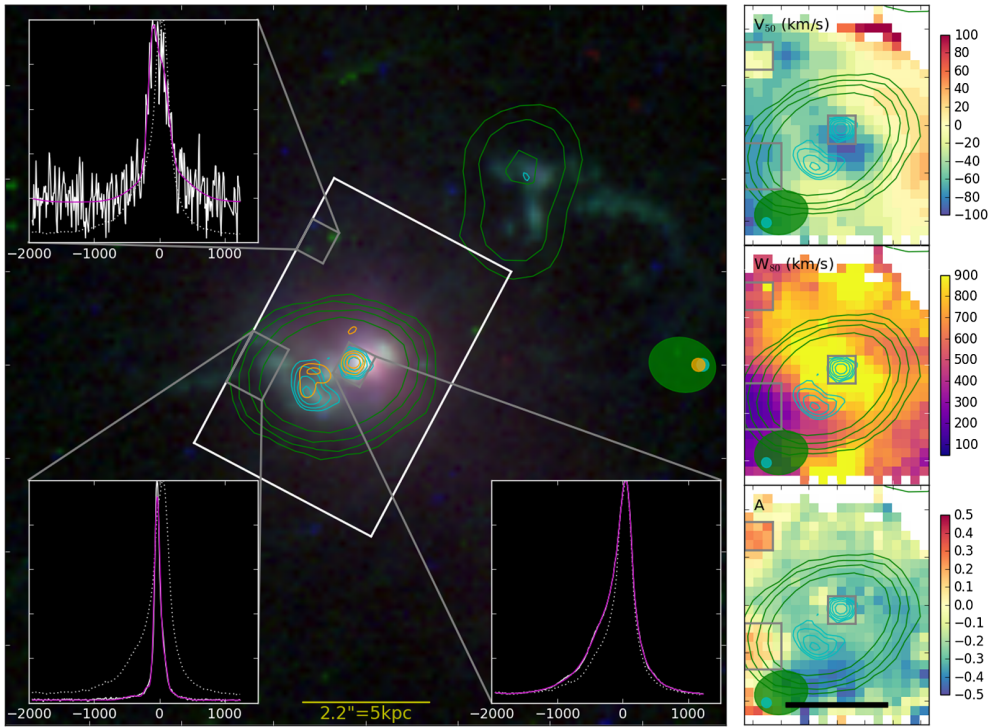
Figure 3. A comparison of the ionized gas and the radio features for J0945+1737. Left: contours from our radio data colour coded as they are in Figure 2 with the beams shown in the middle right, over-layed on HST data with continuum emission in red, [O III] and Hβ in green and H-alpha in blue (proposal id.13741; Cui *et al.* 2001). The FOV of the GMOS IFS is shown in white. [O III]5007 emission line profiles from the grey regions are shown each corner. The weighted average in the box is shown in white, the fit in magenta and the total over the cube as a dotted white line, all normalised to 1 and with the velocity given in km/s. Right: maps of the median velocity (v_{50}), line width (w_{80}) and asymmetry (A; see Harrison *et al.* 2014) with the boxes from the main panel overlayed. The scalebar is the same as in the main panel. The interactions between the radio jet features and the ionised gas are clearly visible.

References

Abazajian, K. N., Adelman-McCarthy, J. K., Agueros, M. A., *et al.* 2009, *ApJS*, 182, 543

An, T. & Baan, W. A. 2012, *ApJ*, 760, 77

Becker, R. H., White, R. L., & Helfand, D. J. 1995, *ApJ*, 450, 559

Bell, E. F. 2003, *ApJ*, 586, 794

Best, P. N. & Heckman, T. M. 2012, *MNRAS*, 421, 1569

Condon, J. J., Kellermann, K. I., Kimball, A. E., Ivezic, ., & Perley, R. A. 2013, *ApJ*, 768, 37

Cui, J., Xia, X.-Y., Deng, Z.-G., Mao, S., & Zou, Z.-L. 2001, *AJ*, 122, 63

Fabian, A. C. 2012, *ARAA*, 50, 455

Harrison, C. M., Alexander, D. M., Mullaney, J. R., & Swinbank, A. M. 2014, *MNRAS*, 441, 3306

Harrison, C. M., Thomson, A. P., Alexander, D. M., *et al.* 2015, *ApJ*, 800, 45

Heckman, T. M., & Best, P. N. 2014, *ARAA*, 52, 589

Jarvis, M. E. *et al.* 2019, *MNRAS*, 485, 2710

Leipski, C. & Bennert, N. 2006, *A&A*, 448, 165

Mullaney, J. R., Alexander, D. M., Fine, S., *et al.* 2013, *MNRAS*, 433, 622

Noll, S., Burgarella, D., Giovannoli, E., *et al.* 2009, *A&A*, 507, 1793

Xu, C., Livio, M., & Baum, S. 1999, *AJ*, 118, 1169

Zakamska, N. L. & Greene, J. E. 2014, *MNRAS*, 442, 784